Published September 1, 1974

ELECTRON MICROSCOPE STUDY OF MITOCHONDRIAL 60S AND CYTOPLASMIC 80S RIBOSOMES FROM *LOCUSTA MIGRATORIA*

W. KLEINOW, W. NEUPERT, and F. MILLER

From the Institut für Physiologische Chemie und Physikalische Biochemie, and the Institut für Zellbiologie, Universität München, 8 München 2, Germany

ABSTRACT

Purified mitochondrial ribosomes (60S) have been isolated from locust flight muscle. Purification could be achieved after lysis of mitochondria in 0.055 M $MgCl_2$. Mitochondrial 60S and cytoplasmic 80S ribosomes were investigated by electron microscopy in tissue sections, in sections of pellets of isolated ribosomes, and by negative staining of ribosomal suspensions. In negatively stained preparations, mitochondrial ribosomes show dimensions of ~270 × 210 × 215 Å; cytoplasmic ribosomes measure ~295 × 245 × 255 Å. From these values a volume ratio of mitochondrial to cytoplasmic ribosomes of 1:1.5 was estimated. Despite their different sedimentation constants, mitochondrial ribosomes after negative staining show a morphology similar to that of cytoplasmic ribosomes. Both types of particles show bipartite profiles which are interpreted as "frontal views" and "lateral views." In contrast to measurements on negatively stained particles, the diameter of mitochondrial ribosomes in tissue sections is ~130 Å, while the diameter of cytoplasmic ribosomes is ~180–200 Å. These data suggest a volume ratio of mitochondrial to cytoplasmic ribosomes of 1:3. Subunits of mitochondrial ribosomes (40S and 25S) were obtained by incubation under dissociating conditions before fixation in glutaraldehyde. After negative staining, mitochondrial large (40S) subunits show rounded profiles with a shallow groove on a flattened side of the profile. Mitochondrial small subunits (25S) display elongated, triangular profiles.

INTRODUCTION

We have described the isolation of ribosomes from the mitochondria of thoracic muscle of *Locusta migratoria* (1, 2). These ribosomes carry nascent peptide chains into which radioactive amino acids are incorporated in vitro as well as in vivo in the presence of cycloheximide (1, 2). The ribosomes show a sedimentation constant of about 60S with all preparative and analytical methods used in our experiments, provided that a dissociation into subunits was avoided. In magnesium-free gradients the ribosomes dissociate into subunits with sedimentation constants of 40S and 25S (2). After dissociation the 40S subunits carry nascent peptide chains, a finding characteristic for large ribosomal subunits (1). RNA species with apparent mol wt of 520,000 and 280,000 could be isolated from the

Downloaded from jcb.rupress.org on November 10, 2008

Published September 1, 1974

40S and 25S subunits, respectively, as well as from the 60S ribosomes and from whole purified mitochondria (3, 4). The proteins from the 40S and 25S subunits display different electrophoretic patterns (2). The mitochondrial ribosomes constitute 2–5% of total cellular ribosomes. They can be clearly distinguished from cytoplasmic ribosomes by sedimentation velocity, size of ribosomal RNA, protein composition, and sensitivity against chloramphenicol and cycloheximide (1, 2, 4). In this paper we report that mitochondrial ribosomes, despite their unusual low sedimentation constant, show morphological features very similar to those of undissociated 80S cytoplasmic ribosomes from the same tissue.

MATERIALS AND METHODS

Preparation of Ribosomes

Locust thoracic muscle mitochondria were prepared and purified as described (2). The mitochondria were suspended in a buffer containing 0.1 M NH_4Cl, 0.1 M $MgCl_2$ and 0.03 M Tris-HCl, pH 7.6. Lysis was performed in 0.055 M $MgCl_2$ by adding the same volume of 5% Triton X-100 in AMT.[1] Concentration of mitochondria during lysis was 2.0–2.5 mg mitochondrial protein/ml. In other experiments lysis was performed in 2.5% Triton X-100 in a buffer containing 0.3 M NH_4Cl, 0.01 M $MgCl_2$, and 0.03 M Tris-HCL, pH 7.6. In this case the lysate was kept frozen over night at −80°C. After a clarifying spin (30 min at 24,000 *g*) the ribosomes were sedimented by centrifuging for 90 min at 144,000 *g*. The crude ribosomal pellets were resuspended in AMT. After a further clarifying spin (10 min at 24,000 *g*) the ribosomal suspensions were placed on top of sucrose gradients made up as described (1, 5) and centrifuged for 5 h at 286,000 *g*. The contents of the tubes were pumped through a 5-mm flow cell (50-μl volume). The absorbance at 260 nm was recorded with a Zeiss PMQ II spectrophotometer (Carl Zeiss, Inc., Oberkochen, W. Germany) and fractions of 0.39 ml were collected with a LKB Ultrorac (LKB Produkter, Stockholm, Sweden). The gradients were fractionated and the absorbancy at 260 nm was recorded. The fractions containing the 60S peak were pooled and dialysed for 16–18 h against a buffer containing 1 M methanol, 0.002 M $MgCl_2$ and 0.03 M Tris-HCl, pH 7.6 (6). All steps of the preparation were carried out between 0°–4°C.

For the preparation of fixed subunits, mitochondrial ribosomes were dissociated by incubation for 5 min either at 37°C in a magnesium-free buffer or at 4°C in a buffer containing no magnesium but 4 mM EDTA. Immediately before gradient centrifugation, 0.2 ml of ribosomal suspension containing ca. 2.0 absorbancy 260-nm units of ribosomal material was mixed with 2 vol of the fixative (7). The fixative was prepared just before use by adding 1 ml 25% glutaraldehyde to 6 ml AMT and 3 ml 1 M Tris. Centrifugation was performed as in the case of 60S ribosomes except that the gradients contained no magnesium. The fractions containing the 40S and the 25S subunits were collected separately and dialysed as described for the undissociated ribosomes. Fixed 60S ribosomes were prepared likewise except that the incubation, before fixation and gradient centrifugation, was omitted.

Cytoplasmic ribosomes were prepared as reported previously (2). The 80S-region from the gradient was collected and dialysed as described for mitochondrial ribosomes. For negative staining, the optical density of the preparations was adjusted to 0.2–0.4 A_{260}-units/ml with dialysis buffer.

Fixation of Muscle Tissue and Ribosomal Pellets

Dorsal median longitudinal flight muscles of *L. migratoria* 1–3 days after imaginal molt were fixed *in situ* in a slightly stretched state in 3% glutaraldehyde in 0.1 M cacodylate buffer, pH 7.3. The tissues were transferred to fresh fixative after hardening for 24–36 h, rinsed overnight in cacodylate buffer containing 0.22 M sucrose, and postfixed in 2% OsO_4 in 0.1 M cacodylate buffer, pH 7.3, for 1 h. Pieces of muscle were also fixed in buffered potassium permanganate (8), pH 6.8, for 2 h.

Small isolated bundles of muscle fibers were fixed for 2 h in 4% formaldehyde (freshly prepared from paraformaldehyde) in 0.1 M Sörensen phosphate buffer, pH 7.2, rinsed for 1 h in the same buffer, incubated in 0.1% RNase (Boehringer and Soehne, Mannheim, W. Germany), pH 6.5, at room temperature for 1.5 h, rinsed in 5% TCA for 30 min at 4°C, and washed in distilled water.

To obtain ribosomal pellets, 60S and 80S ribosomes were collected from sucrose gradients diluted 20-fold with AMT and centrifuged at 144,000 *g* for 2 h. The pellets were fixed in 2% OsO_4 in distilled water. All samples were dehydrated in ethanol and embedded in Epon 812 (9). Thin sections were cut on a LKB-ultrotome III (LKB Produkter, Stockholm, Sweden) with diamond knives, collected on grids covered with parlodion and carbon films, and stained with 7% magnesium uranyl acetate (10) and lead citrate (11).

Negative Staining

Holey parlodion films were prepared after Drahoš and Delong (12), picked up on 300-mesh copper grids, and reinforced by a thick layer of carbon. The grids were

[1] *Abbreviations used in this paper:* AMT, buffer made of 0.1 M ammonium chloride, 0.01 M magnesium chloride, 0.03 M Tris-HCl, pH 7.6; EDTA, ethylene diamine tetraacetate; TCA, trichloroacetic acid.

Downloaded from jcb.rupress.org on November 10, 2008

Published September 1, 1974

recovered with a second parlodion film and a thin layer of carbon was again evaporated at 10^{-5} torr onto them. The grids were then rinsed for 2 days in amylacetate to remove the parlodion films. A drop of the ribosome suspension was deposited on the grid and removed with filter paper after 1–5 min. A drop of 2% uranyl acetate of uncorrected pH was immediately placed on the grid before the film had dried. 0.5–1.0 μl of 0.015% octadecanol in hexane (wt/vol) was applied to the surface of the stain droplet with a microliter syringe (13) and the stain withdrawn with filter paper. The procedure usually gave a homogeneous distribution of the particles and a good spreading of the stain.

Electron Microscopy

Micrographs were taken in a Siemens Elmiskop 101 operated at 80 KV and equipped with a thin, self-cleaning 50-μm objective aperture and a cooling device, on Ilford EM 6 plates (Ilford Ltd., Ilford Essex, England) at direct magnifications of 10,000–40,000 for sections and 80,000–100,000 for negatively stained material. The specimen side of the grid faced the viewing screen and the plates were printed with the emulsion side facing the bromide paper. The magnification was calibrated with a cross-linked grating replica provided with 2,160 lines/mm (E. Fullam, Schenectady, N.Y.). About 50 measurements were made on prints at a final magnification of 280,000 for each type of particle.

RESULTS

Sedimentation Pattern of Unfixed Ribosomes

Fig. 1 shows gradient profiles (absorbancy at 260 nm) of unfixed ribosomes from locust thoracic muscle. In Fig. 1 A a preparation of mitochondrial ribosomes is shown which was obtained after lysis of mitochondria in AMT (2). The 60S peak contains the undissociated 60S ribosomes; in addition, a small amount of 40S subunits is present. The ribosomes in the 60S peak are contaminated by a protein particle which was described previously and called "Mx" (2). Therefore procedures were developed in order to prepare mitochondrial ribosomes free of the contaminating protein.

The mitochondrial ribosomes shown in the gradient in Fig. 1 B were obtained after lysis of mitochondria in 0.055 M $MgCl_2$. In this gradient the mitochondrial ribosomes appear to be partially dissociated. Three peaks are prominent. The 60S peak represents the undissociated mitochondrial ribosome; the 40S and 25S peaks correspond to the large and small subunits.

The subunit peaks are much higher than in the

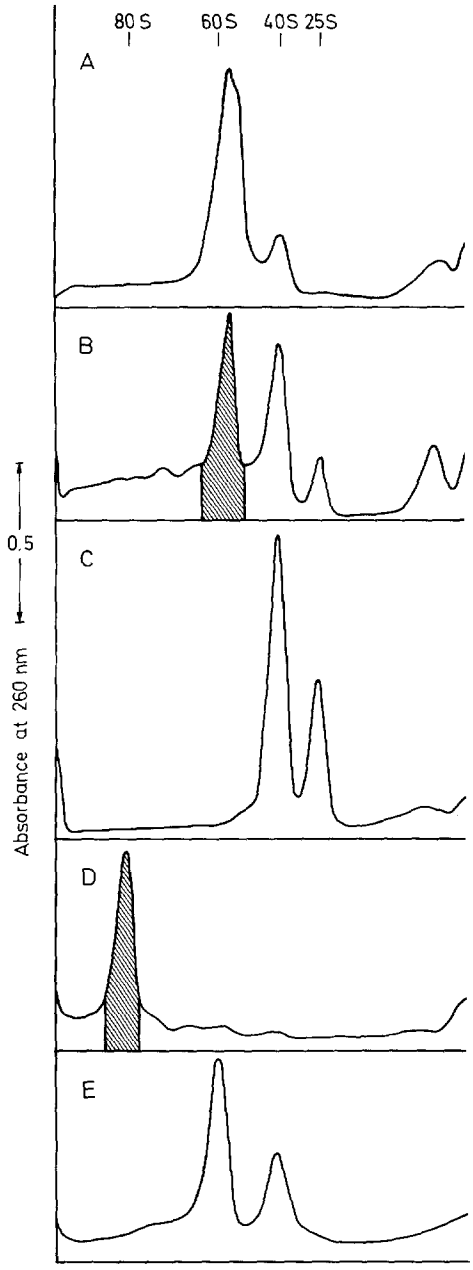

FIGURE 1 Gradient profiles of unfixed mitochondrial and cytoplasmic ribosomes. The shadowed areas represent material used for electron microscopy. (A) Mitochondrial ribosomes prepared after lysis of mitochondria in AMT (magnesium containing gradient). (B) Mitochondrial ribosomes prepared after lysis of mitochondria in 0.055 M $MgCl_2$ (magnesium containing gradient). (C) Mitochondrial ribosomes prepared after lysis of mitochondria in 0.055 M $MgCl_2$ (magnesium-free gradient). (D) Cytoplasmic ribosomes (magnesium containing gra-

Downloaded from jcb.rupress.org on November 10, 2008

Published September 1, 1974

gradient shown in Fig. 1 A. The protein contamination Mx is greatly diminished by this procedure. This is shown more clearly in Fig. 1 C. In this case, mitochondrial ribosomes prepared after lysis of mitochondria in 0.055 M $MgCl_2$ were centrifuged on a magnesium-free gradient. The ribosomes are completely dissociated and no Mx is present in the 60S region. If, on the other hand, ribosomes prepared as in Fig. 1 A are centrifuged in a magnesium-free gradient, the particle Mx still appears in the 60S region (2).

Gradient profiles of ribosomes obtained from lysates of mitochondria after freezing at −80°C in 0.3 M NH_4Cl are similar to the profile shown in Fig. 1 B. The absence of Mx could also be demonstrated.

Cytoplasmic ribosomes are shown in Fig. 1 D and E. In a magnesium-containing gradient, essentially one peak is visible (Fig. 1 D). It represents the 80S cytoplasmic ribosomes. In a magnesium-free gradient (Fig. 1 E) the cytoplasmic ribosomes dissociate into the 60S and 40S subunits. The material used for electron microscope examination is marked by the shadowed areas in Fig. 1 B and D.

The degree of purification of the different ribosomal preparations was also checked by recording the absorption spectra between 320 and 230 nm. In Table I the absorption ratios of mitochondrial and cytoplasmic ribosomes at 260 nm/280 nm and 260 nm/240 nm are listed for different steps of the purification procedure. The relative absorbancy at 280 nm depends on the amount of protein associated with the ribosomes. The absorbancy around 240 nm is also a measure of the protein content (14); in addition, aggregation of ribosomes and contamination with membrane fragments and with residual Triton X-100 may increase the absorption in this region. As can be seen from Table I, the absorption ratios of mitochondrial ribosomes prepared in 0.055 M $MgCl_2$ approach those of cytoplasmic ribosomes. In contrast, mitochondrial ribosomes prepared by lysis in AMT display much lower ratios. In all cases gradient centrifugation improves the purity.

Sedimentation Pattern of Fixed Ribosomes

For the demonstration of ribosomal subunits by negative staining, the particles were treated with glutaraldehyde before centrifugation. This was done because it was observed that unfixed subunits tend to clump together on the grid. With regard to undissociated mitochondrial ribosomes no difference in morphology between unfixed and fixed particles was observed; hence, we assume that this holds true also for isolated subunits.

Gradients of fixed mitochondrial ribosomes are shown in Fig. 2. In these experiments the ribosomes were prepared in 0.055 M $MgCl_2$ and centrifuged in magnesium-free gradients. The ribosomes in Fig. 2 A were treated with glutaraldehyde

dient). (E) Cytoplasmic ribosomes (magnesium-free gradient).

TABLE I

Spectral Data of Ribosomal Suspensions after Different Purification Steps

	Mitochondrial Ribosomes		Cytoplasmic Ribosomes	
	260/280	260/240	260/280	260/240
Crude ribosomes after lysis in medium containing 0.055 M $MgCl_2$	1.76 ± 0.11*	1.35 ± 0.14	Not determined	
Crude ribosomes after lysis in medium containing 0.01 M $MgCl_2$	1.48 ± 0.14	1.15 ± 0.12	1.79 ± 0.09	1.38 ± 0.12
Ribosomes from gradient after lysis in 0.055 M $MgCl_2$	1.73 ± 0.15	1.68 ± 0.19	Not determined	
Ribosomes from gradient after lysis in 0.01 M $MgCl_2$	1.64 ± 0.14	1.15 ± 0.28	1.98 ± 0.11	1.30 ± 0.30

Absorbancy ratios of 260 nm : 280 nm and 260 nm : 240 nm were calculated from spectra recorded with a Beckman DK 1A spectrophotometer (Beckman Instruments, Inc., Fullerton, Calif.)

* Standard deviation.

Downloaded from jcb.rupress.org on November 10, 2008

Published September 1, 1974

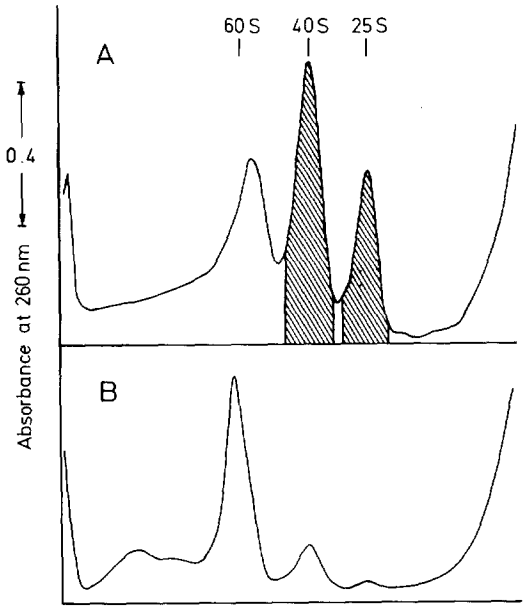

FIGURE 2 Gradient profiles of fixed mitochondrial ribosomes. The ribosomes were prepared after lysis of mitochondria in 0.055 M $MgCl_2$; the gradients contained no magnesium. The shadowed areas represent material used for electron microscopy. (A) Ribosomes were resuspended in 0.004 M EDTA before treatment with glutaraldehyde. (B) Ribosomes were resuspended in AMT before treatment with glutaraldehyde.

after incubation under dissociating conditions (see Material and Methods), whereas in Fig. 2 B such an incubation step was omitted. Gradient centrifugation of ribosomes treated in the first way resolves subunits which were used for electron microscope studies. The efficiency of the fixation procedure is demonstrated by centrifugation of ribosomes which were treated with the fixative under nondissociating conditions; in this case, essentially 60S ribosomes are present in the gradient (Fig. 2 B). This is in contrast to unfixed mitochondrial ribosomes which are completely dissociated under such conditions (Fig. 1 C).

The experiment in Fig. 2 B illustrates also that the preparation of mitochondrial ribosomes in 0.055 M $MgCl_2$ does not lead by itself to the marked dissociation into subunits observed in Fig. 1 B. It has to be assumed that treatment in 0.055 M $MgCl_2$ renders the association between the subunits less stable, so that the hydrostatic pressure during centrifugation can result in the dissociation into subunits. The incubation of ribosomes under dissociating conditions before fixation and gradient centrifugation apparently does not lead to complete dissociation (Fig. 2 A). This is in contrast to the complete dissociation after centrifugation of unfixed ribosomes in magnesium-free gradients (Fig. 1 C).

Ribosomes in Sections of Muscle Tissue

Cytoplasmic ribosomes (mean diameter: ~180–200 Å) lie between the myofibrils and are densely packed around mitochondria (Fig. 3). Mitochondrial ribosomes (Fig. 3) are smaller (mean diameter ~130 Å) and scattered irregularly in the matrix; they are quite numerous, but show no preferential arrangement along mitochondrial membranes. Glycogen particles (mean diameter ~ 230 Å) are located between the myofilaments of the I-band at both sides of the Z-line. In tissue fixed in potassium permanganate or digested with RNase (Fig. 4) the cytoplasmic and mitochondrial ribosomes are not visible.

Pellets of Isolated Ribosomes

Sections of cytoplasmic (Fig. 5) and mitochondrial (Fig. 6) ribosomal pellets show a homogeneous distribution of particles without contamination by other cell constituents. The particles are slightly larger than in tissue sections, possibly because they are not constrained by other tissue components during fixation. The mean diameter of cytoribosomes is ~ 200 Å, of mitoribosomes ~ 180 Å.

Morphology of Negatively Stained Ribosomes

CYTORIBOSOMES FROM THE 80S PEAK: Among the variety of roundish and oval profiles (Fig. 7), several predominate; selected examples are shown in Fig. 8.

Form F is often observed and has an oval outline. A dense band separates partially or completely two parts of different size (Fig. 8) which correspond to ribosomal subunits. The small subunit is oblong and slightly curved; the large subunit is triangular with curved sides, and the base of the triangle faces the concave side of the small subunit. The small subunit is sometimes partitioned in two parts of different size by a faint dense line (Fig. 8) perpendicular to the band separating the small from the large subunit; where this faint line abuts on the horizontal band, a dense spot is found off center with equal frequency to the left or to the

Downloaded from jcb.rupress.org on November 10, 2008

Published September 1, 1974

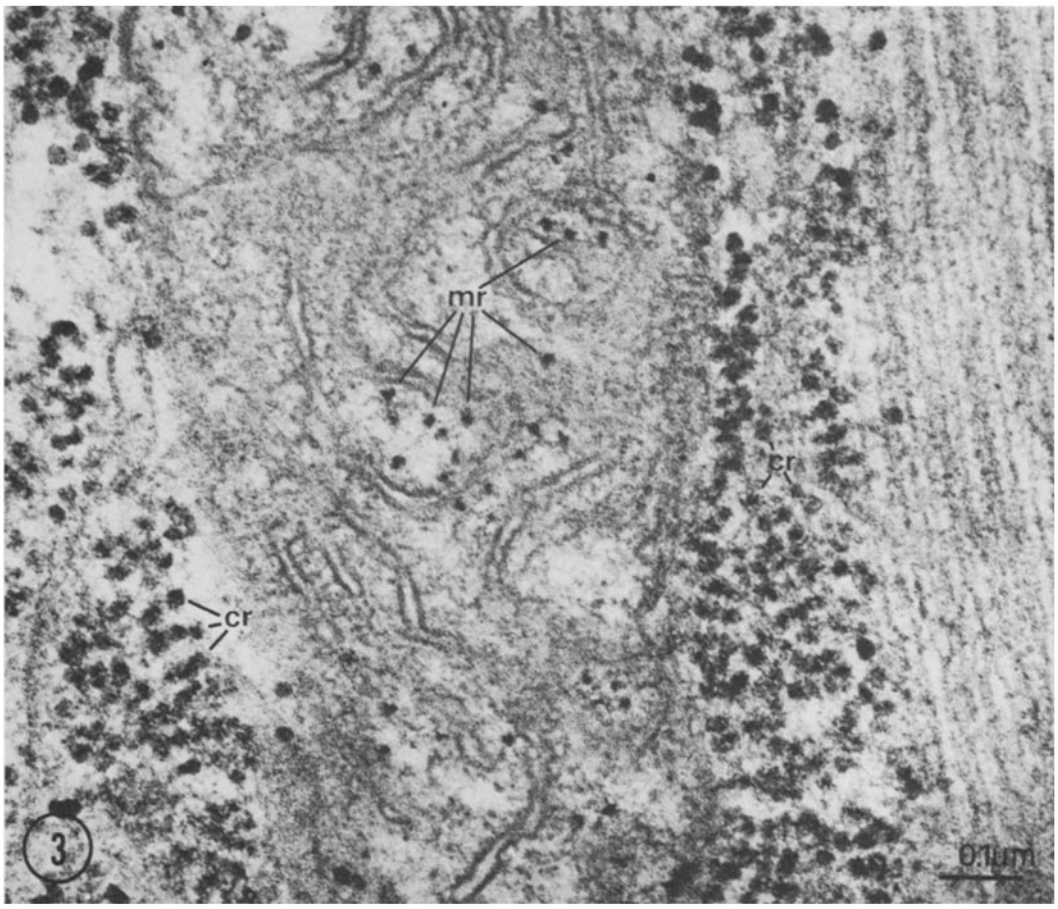

FIGURE 3 Section of locust flight muscle. Numerous mitoribosomes (*mr*) are scattered irregularly in the matrix of a mitochondrion surrounded by cytoribosomes (*cr*) on both sides. Myofilaments are at right. Uranyl- and lead-stained. × 112,000.

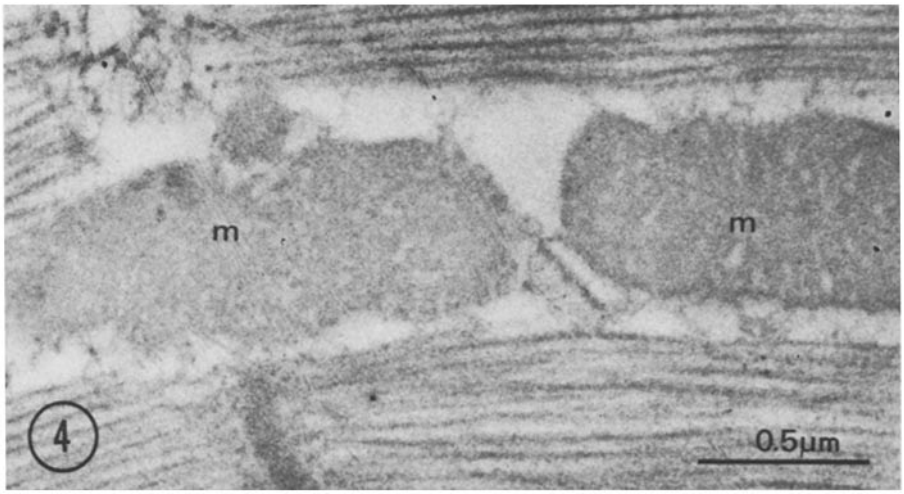

FIGURE 4 Section of locust flight muscle incubated in 0.1% RNase, fixed in formaldehyde, and stained with uranyl and lead. Ribosomes are no longer visible in mitochondria (*m*) and in the surrounding cytoplasm. × 45,000.

Downloaded from jcb.rupress.org on November 10, 2008

Published September 1, 1974

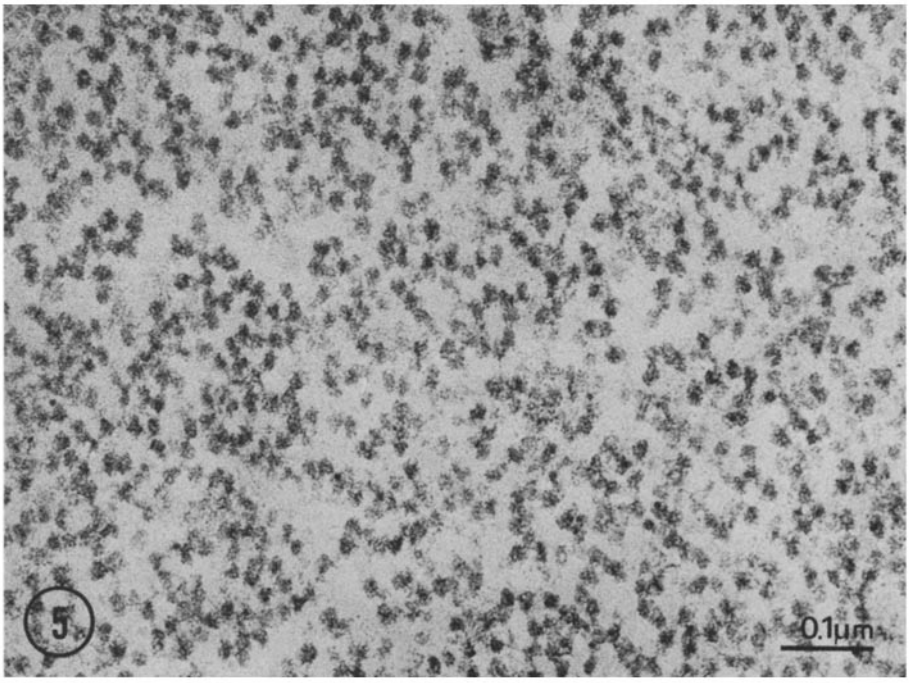

FIGURE 5 Section of pellet of cytoribosomes. Uranyl- and lead-stained. × 120,000.

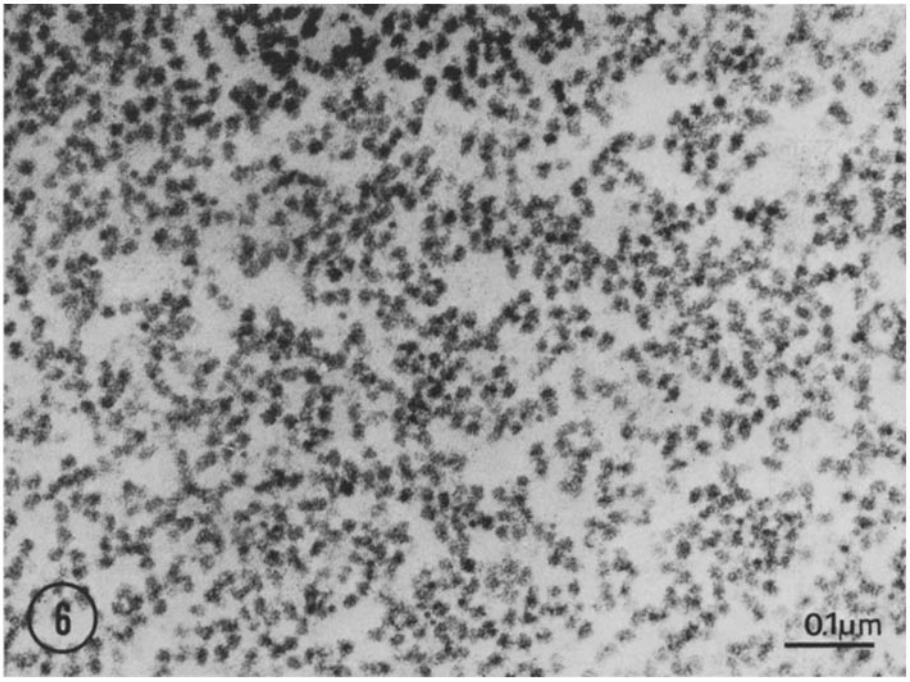

FIGURE 6 Section of a pellet of mitoribosomes. Uranyl- and lead-stained. × 120,000.

Downloaded from jcb.rupress.org on November 10, 2008

Published September 1, 1974

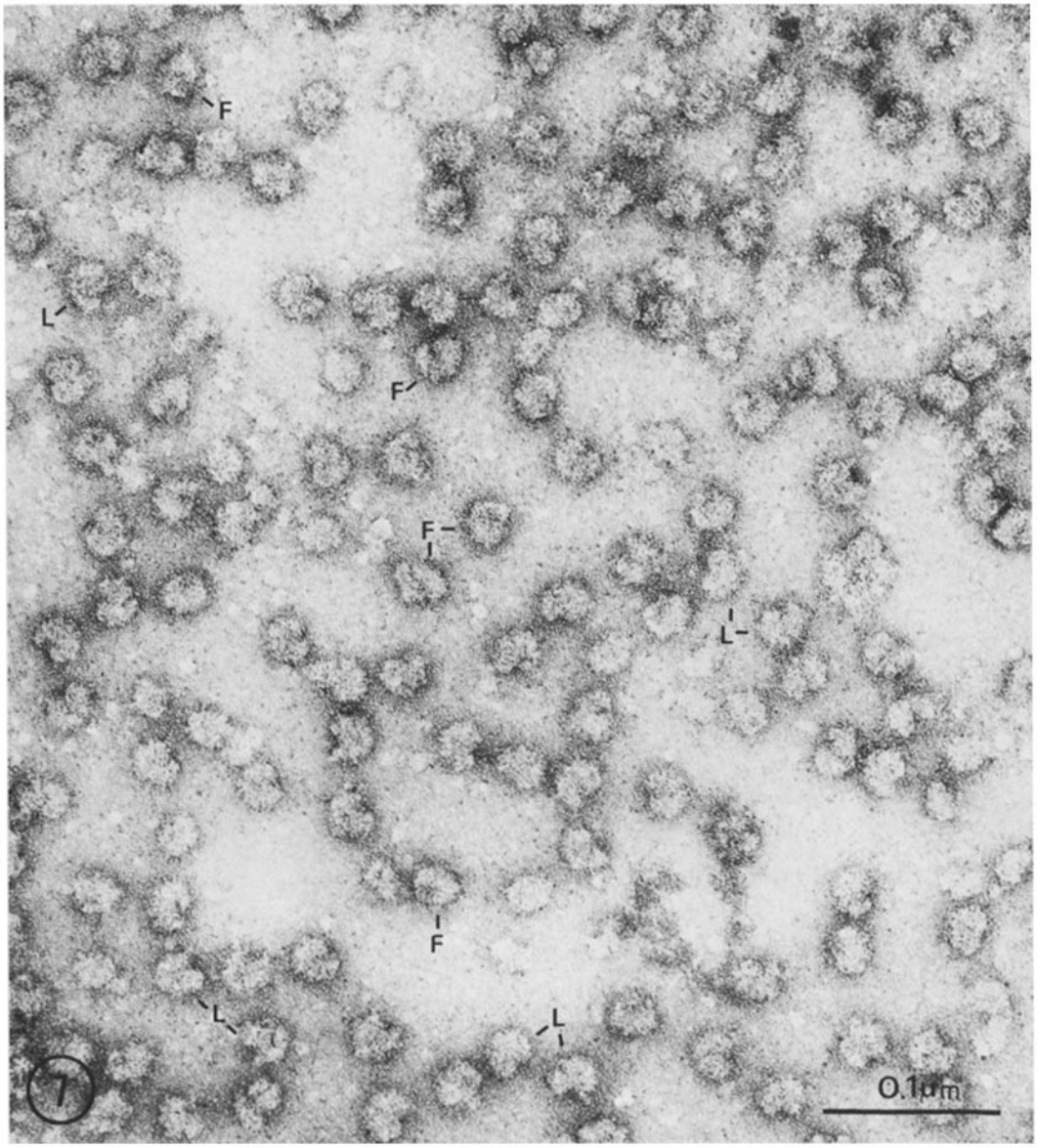

FIGURE 7 General view of a field of negatively stained cytoribosomes (80S). Forms *F* and *L* are indicated. × 240,000.

right side of the ribosome if the latter is so arranged that the tip of the large subunit points downwards (Fig. 8).

These two aspects of form F correspond in most details to the forms of cytoribosomes in rat liver described by Nonomura et al. (15) as "left" and "right-featured frontal" images.

Form L (Figs. 7, 8) corresponds to the right lateral and left lateral views of the ribosomes as described by Nonomura et al. (15). Two segments are visible in these cases. The smaller one is either angular or roundish; the larger one is shaped like the hull of a boat and joins the base of the smaller segment with its upper side. The small subunit is displaced either to the right or to the left side of the large subunit if the latter is oriented with its tip

Downloaded from jcb.rupress.org on November 10, 2008

Published September 1, 1974

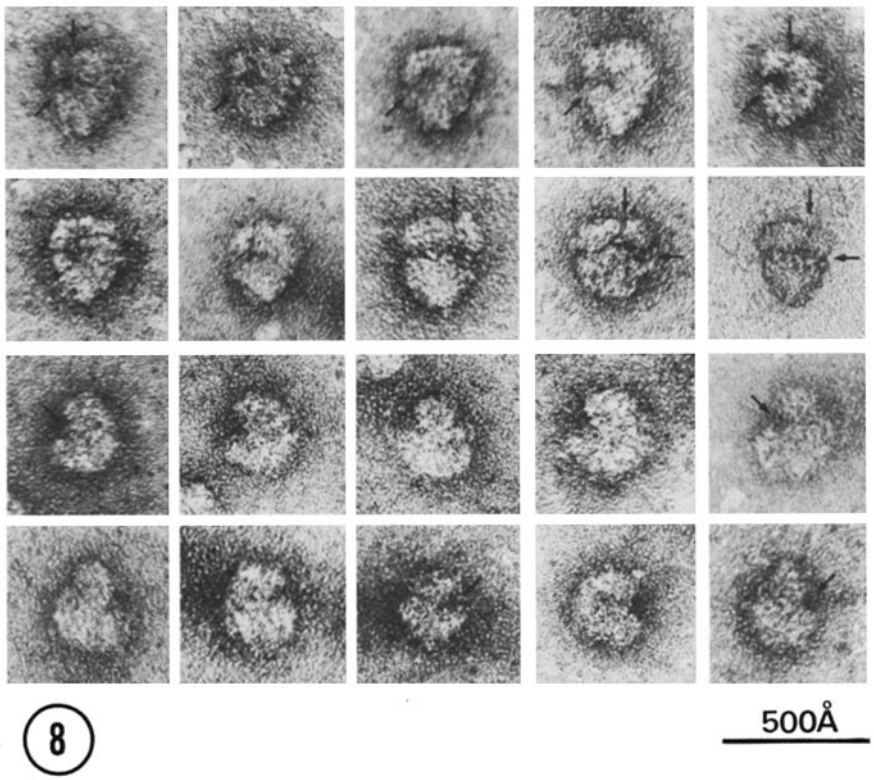

FIGURE 8 Selected images of cytoribosomes. The images of the first row and the first two images of the second row are left-featured; the last three images of the second row are right-featured frontal images. The third row shows right-lateral, and the fourth row left-lateral images. The vertical arrows (first and second row) point to the partition in the small subunit. The horizontal and oblique arrows point to the dense spot located between the subunits in frontal images or in front of the small subunit in lateral images. The horizontal dense band between large and small subunit is clearly visible in the right featured frontal images. × 400,000.

pointing downwards. The two forms are enantiomorphic and occur with equal frequency. No partition is visible in the small subunit; a stain-filled notch is frequently present in the middle of the base of the large subunit, where it is joined to the small subunit (Fig. 8).

A few other profiles are present in the fields which may correspond to "top" views as described by Vignais et al. (16). However, an unambiguous interpretation is difficult and must await the results of tilting experiments in progress.

MITORIBOSOMES FROM THE 60S PEAK: Two main forms are also found in mitoribosomal preparations (Figs. 9, 10). Form F is observed frequently and differs slightly from the corresponding profiles of cytoribosomes. The horizontal band between large and small subunit is not visible across the entire width; it can be followed only from one side to the dense spot located always off center. The band is seen either on the left third or on the right third of the ribosome profile when the tip of the large subunit points downwards. A partition of the small subunit was not observed.

Form L (lateral views) occurs rarely; the two enantiomorphic aspects do not differ significantly from those of cytoribosomes.

The dimensions of negatively stained cyto- and mitoribosomes are summarized in Table II. Mitoribosomes are generally smaller than cytoribosomes, but the difference is less conspicuous than in sections of muscle tissue.

Subunits of Mitoribosomes

The large (40S) subunit (Figs. 11, 12) appears most frequently as a roughly triangular profile

Downloaded from jcb.rupress.org on November 10, 2008

Published September 1, 1974

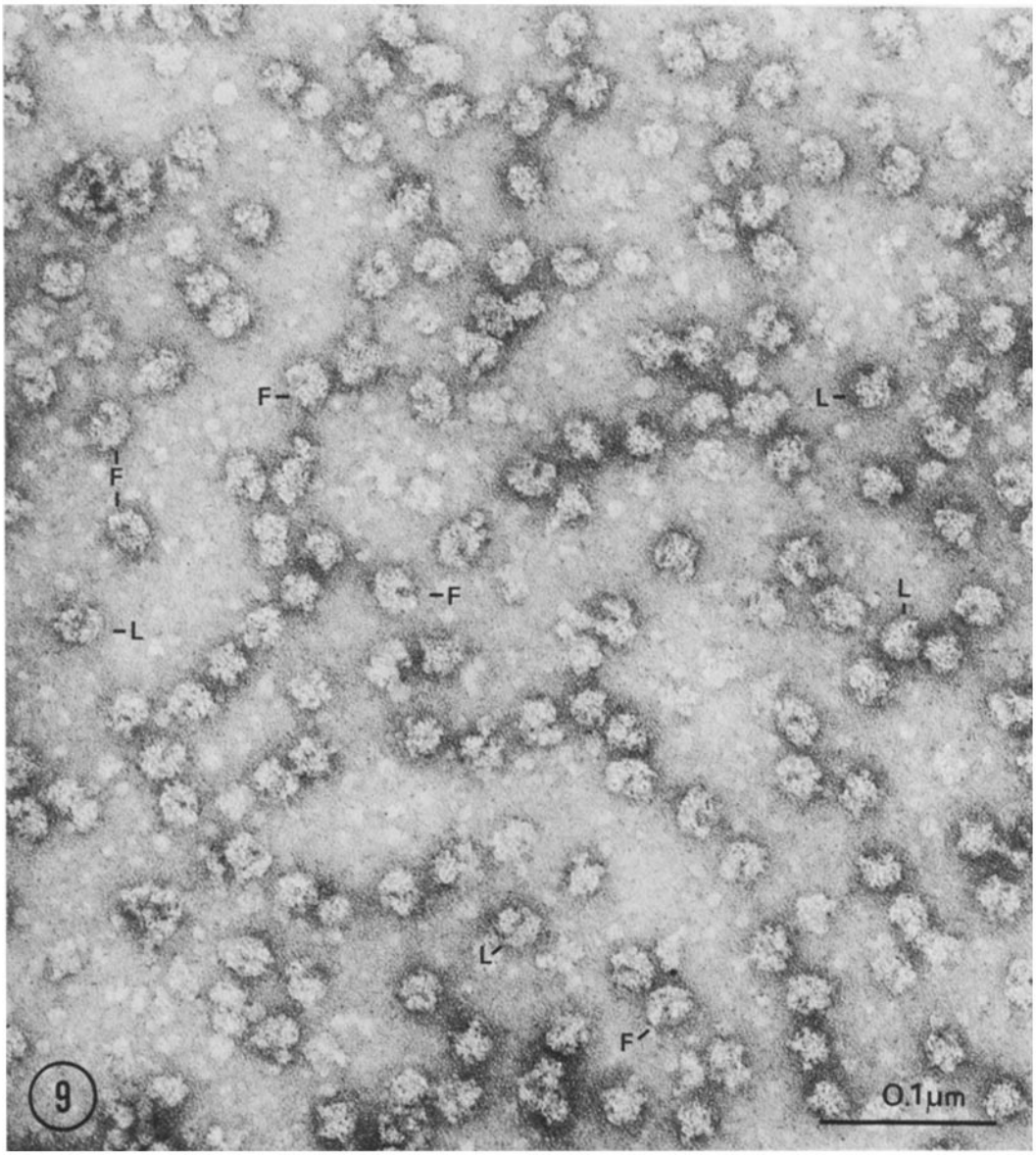

FIGURE 9 General view of a field of negatively stained mitoribosomes (60S). Forms *F* and *L* are indicated. × 240,000.

with curved flanks resembling the hull of a boat. In Fig. 12 selected images are oriented in such a way that the side connecting to the small subunit in undissociated ribosomes faces upwards; this side is slightly concave and stain accumulates sometimes in a shallow groove. Roughly circular profiles also occur.

The small (25S) subunit (Figs. 13, 14) is an elongate, roughly triangular and often slightly curved particle with one pointed and one blunter end. One side is often convex and the other flat or concave. Particles with approximately rectangular circumference also occur.

DISCUSSION

Our results show that mitochondrial ribosomes from *Locusta*, in contrast to their low sedimentation constant of 60S, reveal morphological fea-

Downloaded from jcb.rupress.org on November 10, 2008

Published September 1, 1974

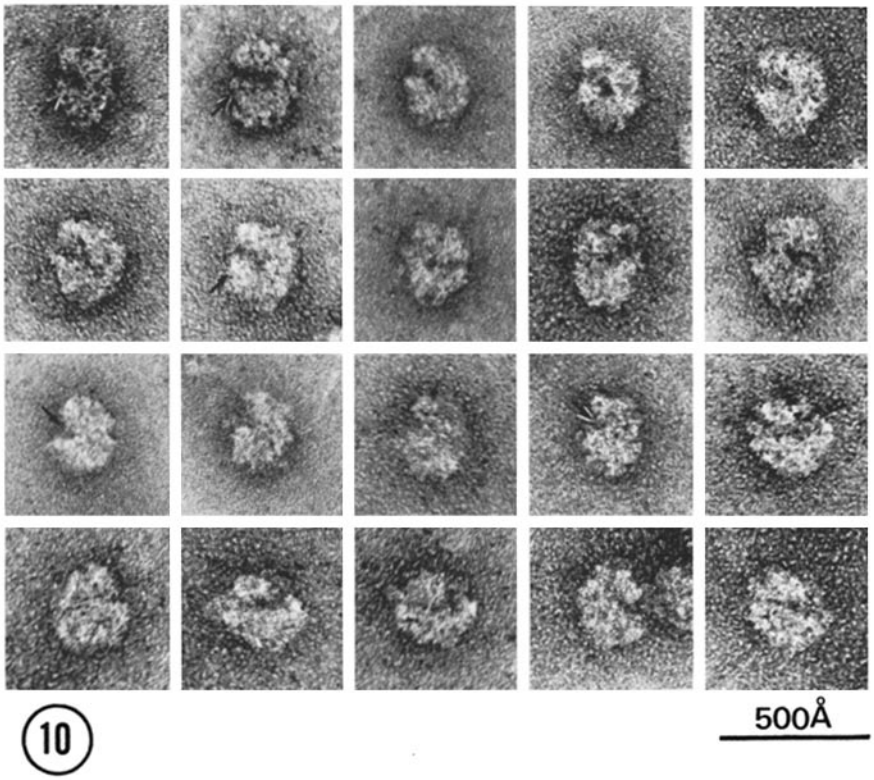

FIGURE 10 Selected images of mitoribosomes. The images of the first row and the first two images of the second row are left-featured; the last three images of the second row are right-featured frontal images. The third row shows right-lateral, and the fourth row left-lateral images. The oblique arrows point to the dense spot located between the subunits in frontal images or in front of the small subunit in lateral images. × 400,000.

TABLE II

Dimensions of Negatively Stained Ribosomes from Locusta migratoria Thoracic Muscle

	Cytoribo-somes	Mitoribo-somes
Frontal view		
Total height	294 ± 18	271 ± 18
Height of large subunit	185 ± 16	159 ± 16
Height of small subunit	106 ± 15	103 ± 13
Width along the cleft between the subunits	245 ± 21	210 ± 18
Lateral view		
Total height	294 ± 22	268 ± 25
Height of large subunit	191 ± 16	157 ± 23
Height of small subunit	104 ± 16	110 ± 19
Width of large subunit	257 ± 16	215 ± 28
Width of small subunit	145 ± 19	140 ± 28

Dimensions ± standard deviation are in angstrom units; 50 measurements were averaged for each value; for lateral views of mitochondrial ribosomes, only 20 measurements were evaluated.

tures which are in general similar to those of other ribosomes studied with the technique of negative staining (15–18). The pictures of particles found in negatively stained preparations are projections and depend on the orientation of the particles on the grid. A three-dimensional model of cytoplasmic ribosomes from rat liver has been constructed by means of tilting negatively stained prep rations during the observation in the electron microscope, a procedure which interconverts different projections (15). The finding of similar projections in both cytoplasmic and mitochondrial ribosomes from *Locusta* suggests that this model can also be applied to the cytoplasmic and mitochondrial ribosomes from insects. The similarity between cytoplasmic ribosomes from rat liver and locust muscle seems to be very close. On the other hand, the pictures of the mitochondrial ribosomes, besides showing general similarity, show some differences. Thus, typical lateral views are rare in the mitochondrial preparations. In the frontal views

Downloaded from jcb.rupress.org on November 10, 2008

Published September 1, 1974

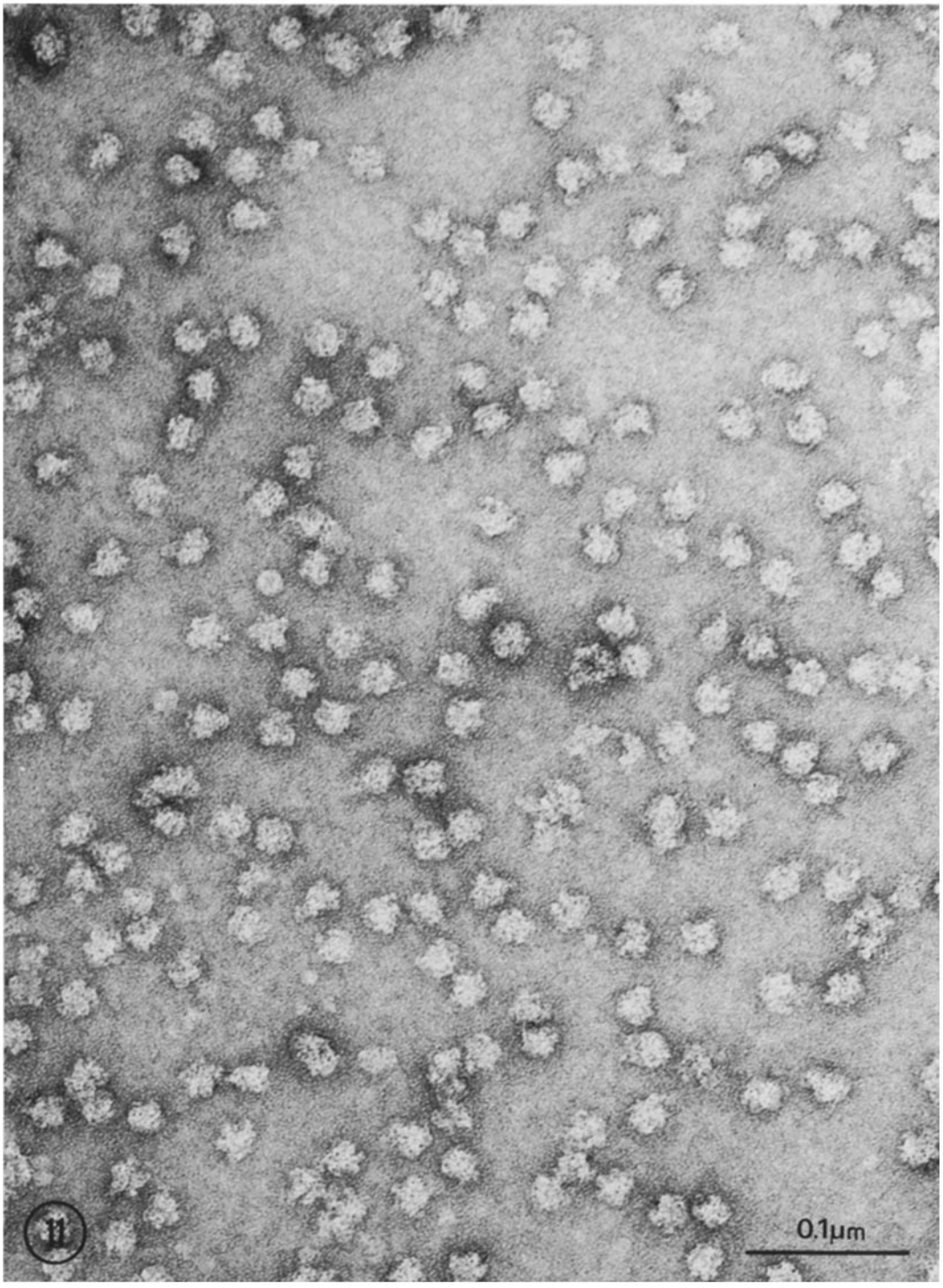

FIGURE 11 General view of a field of negatively stained large mitoribosomal subunits (40S). × 240,000.

Downloaded from jcb.rupress.org on November 10, 2008

Published September 1, 1974

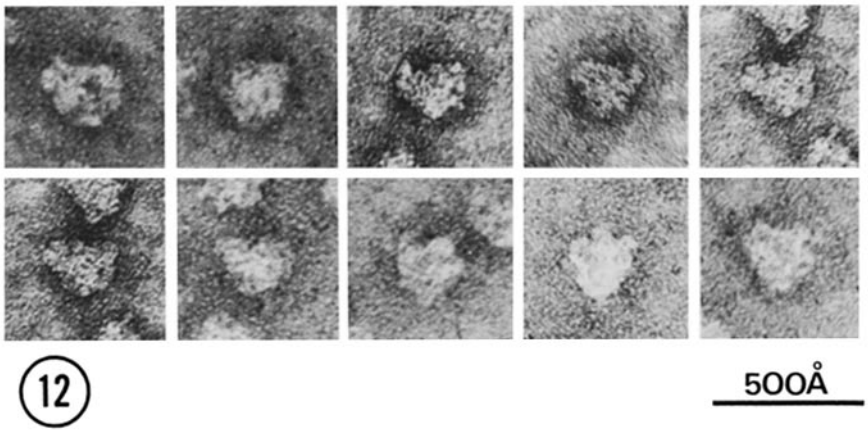

FIGURE 12 Selected images of large mitoribosomal subunits. A shallow groove on the upper side (facing the small subunit) is visible in the last three images of the upper row. × 400,000.

the division between the subunits traverses only one-half of the particle. Negative staining was used in studies of 55S particles from rat liver mitochondria by O'Brien and Kalf (19) and by Aaij et al. (20). The latter authors described a partition interpreted as separation between large and small subunits.

The preparations of negatively stained isolated large and small subunits of mitoribosomes show, first of all, that both particle types from the 40S and from the 25S peak are morphologically distinct and not interconvertible. The shape of the isolated large subunit agrees in general with that of ribosomes from other sources. Rounded or semicircular profiles have been described for the large subunit from rat liver cytoplasmic ribosomes (15, 18) and for mitochondrial ribosomes from yeast (16). We were not able, however, to identify a knoblike projection as described for yeast mitochondrial large subunits (16).

The isolated mitochondrial small subunits show a greater diversity. They have, in common with small ribosomal subunits of other origin, the elongated appearance. The shape of the small mitochondrial subunit, however, differs from that of the small subunits of rat liver cytoplasmic ribosomes (15, 18) as well as from that of the small subunit from *Escherichia coli* ribosomes (21). Besides showing forms resembling the arrowhead-shaped or tetragonal forms found in preparations of yeast mitochondrial subunits (16), the preparations from *Locusta* display most frequently elongated triangular forms. A small subunit partition could not be observed.

Further examinations are necessary to clarify whether this triangular shape of the small subunit is a peculiarity of mitochondrial 60S ribosomes, or whether it is due to artifacts produced during dissociation or fixation.

The comparison of the measurements on negatively stained cytoplasmic and mitochondrial ribosomes from *Locusta* (Table II) shows that the mitochondrial ribosomes are slightly smaller than the cytoplasmic ribosomes. The differences amount maximally to about 10–20% of the linear dimensions of the particles. Planimetry of the pictures of cytoplasmic and mitochondrial ribosomes points to a volume ratio of 1.5:1. This is at variance with the large differences of the sedimentation constants and also with the large differences of the molecular weights of the ribosomal RNA species from cytoplasm and mitochondria (4). On the other hand, the diameters of ribosomal particles found in tissue sections after positive staining show a difference which agrees better with these analytical data. The proportion of the diameters of 180–200:130 corresponds to a ratio of the particle volumes of about 3:1. The diameter of mitoribosomes in tissue sections of vertebrates (22) was also found to be in the same range (120–150 Å) as here described for insects. The difference in size between negatively stained, unfixed particles and positively stained particles after fixation of the whole muscle cannot be explained at the moment.

We wish to thank Miss H. Rothe and Mr. A. Pfaller for excellent technical assistance, and Mrs. L. Döhle and Miss E. Praetorius for help with the photographic work.

Downloaded from jcb.rupress.org on November 10, 2008

Published September 1, 1974

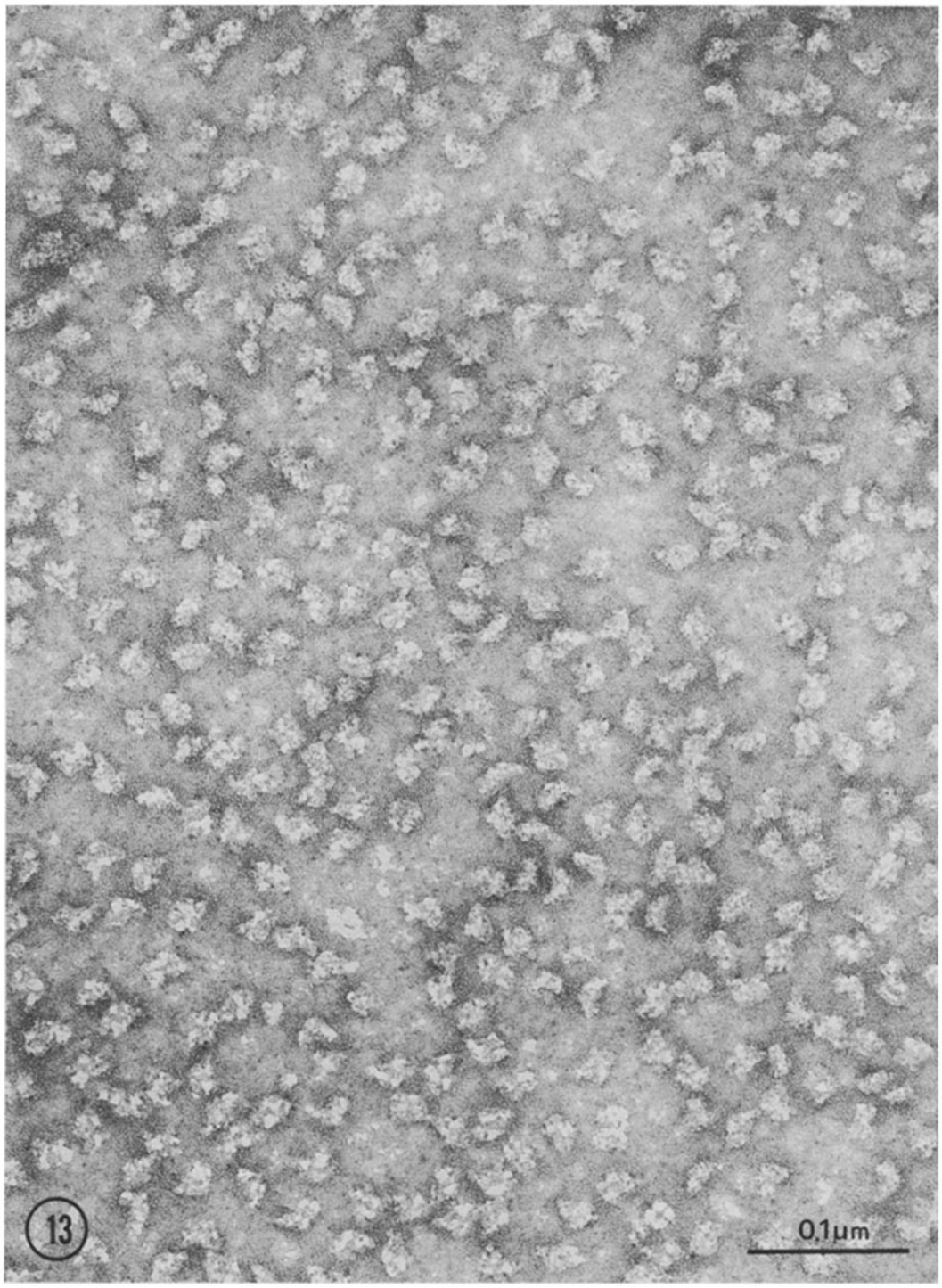

FIGURE 13 General view of a field of negatively stained small mitoribosomal subunits (25S). × 240,000.

Downloaded from jcb.rupress.org on November 10, 2008

Published September 1, 1974

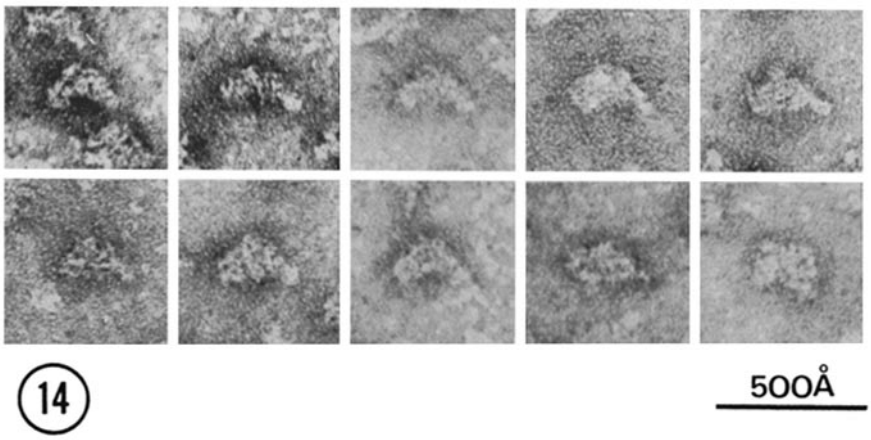

FIGURE 14 Selected images of small mitoribosomal subunits. Most forms are roughly triangular and curved, with one blunt and one more pointed end. The last two images in the second row show a quadrangular profile. × 400,000.

This work was supported by Deutsche Forschungsgemeinschaft, Sonderforschungsbereich 51, and was presented in part at the 66th Meeting of the Deutsche Zoologische Gesellschaft, September 1972 (23), and at the International Conference on the Biogenesis of Mitochondria, June 1973 (24).

Received for publication 3 January 1974, and in revised form 3 May 1974.

REFERENCES

1. KLEINOW, W., W. NEUPERT, and TH. BÜCHER. 1971. Small-sized ribosomes from mitochondria of *Locusta migratoria*. *FEBS* (*Fed. Eur. Biochem. Soc.*) *Lett.* **12**:129–133.
2. KLEINOW, W., and W. NEUPERT. 1971. The mitochondrial ribosome from *Locusta migratoria*: dissociation into subunits. *FEBS* (*Fed. Eur. Biochem. Soc.*) *Lett.* **15**:359–364.
3. KLEINOW, W. 1974. RNA from mitochondrial ribosomes of Locusta migratoria. *In* The Biogenesis of Mitochondria. A. M. Kroon and C. Saccone, editors. Academic Press Inc., New York and London. 377–381.
4. KLEINOW, W., and W. NEUPERT. 1970. RNA aus Mitochondrien des Thoraxmuskels von *Locusta migratoria*. *Z. Physiol. Chem.* **351**:1205–1214.
5. NOLL, H. 1967. Characterization of macromolecules by constant velocity sedimentation. *Nature* (*Lond.*). **215**:360–363.
6. VASILIEV, V. D. 1971. Electron microscopy study of 70S ribosomes of E. coli. *FEBS* (*Fed. Eur. Biochem. Soc.*) *Lett.* **14**:203–205.
7. SUBRAMANIAN, A. R. 1972. Glutaraldehyde fixation of ribosomes. Its use in the analysis of ribosome dissociation. *Biochemistry*. **11**:2710–2714.
8. TAHMISIAN, T. N. 1964. Use of the freezing point method to adjust the tonicity of fixing solutions. *J. Ultrastruct. Res.* **10**:182–188.
9. LUFT, J. H. 1961. Improvements in epoxy resin embedding methods. *J. Biophys. Biochem. Cytol.* **9**:409–414.
10. FRASCA, J. M., and V. R. PARKS. 1965. A routine technique for double-staining ultrathin sections using uranyl and lead salts. *J. Cell Biol.* **25**:157–161.
11. REYNOLDS, E. S. 1963. The use of lead citrate at high pH as an electron-opaque stain in electron microscopy. *J. Cell Biol.* **17**:208–212.
12. DRAHOŠ, V., and A. DELONG. 1960. A simple method for obtaining perforated supporting membranes for electron microscopy. *Nature* (*Lond.*). **186**:104.
13. GORDON, C. N. 1972. The use of octadecanol monolayers as wetting agents in the negative staining technique. *J. Ultrastruct. Res.* **39**:173–185.
14. PETERMANN, M. L. 1964. The physical and chemical properties of ribosomes. Elsevier Publishing Co., Amsterdam, London, New York.
15. NONOMURA, Y., G. BLOBEL, and D. SABATINI. 1971. Structure of liver ribosomes studied by negative staining. *J. Mol. Biol.* **60**:303–324.
16. VIGNAIS, P. V., B. J. STEVENS, J. HUET, and J. ANDRÉ. 1971. Mitoribosomes from *Candida utilis*. Morphological, physical, and chemical characterization of the monomer form and of its subunits. *J. Cell Biol.* **54**:468–492.
17. NANNINGA, N. 1973. Structural aspects of ribosomes. *Int. Rev. Cytol.* **35**:135–188.
18. LUTSCH, G., H. BIELKA, K. WAHN, and J. STAHL. 1972. Studies on the structure of animal ribosomes. III. Electron microscopic investigations of isolated rat liver ribosomes and their subunits. *Acta Biol. Med. Ger.* **29**:851–876.

Downloaded from jcb.rupress.org on November 10, 2008

Published September 1, 1974

19. O'BRIEN, T. W., and G. F. KALF. 1967. Ribosomes from rat liver mitochondria. II. Partial characterization. *J. Biol. Chem.* **242**:2180–2185.
20. AAIJ, C., N. NANNINGA, and P. BORST. 1972. The structure of ribosome-like particles from rat liver mitochondria. *Biochim. Biophys. Acta.* **227**: 140–148.
21. WABL, M. R., P. J. BARENDS, and N. NANNINGA. 1973. Tilting experiments with negatively stained *E. coli* ribosomal subunits. An electron microscopic study. *Cytobiologie.* **7**:1–9.
22. ANDRÉ, J., and V. MARINOZZI. 1965. Présence, dans les mitochondries, de particules ressemblant aux ribosomes. *J. Microsc. (Paris).* **4**:615–626.
23. KLEINOW, W., W. NEUPERT, and F. MILLER. 1973. Untersuchungen zur Cytotopik und Struktur der Proteinsynthese-Systeme in der Thoraxmuskulatur von *Locusta migratoria*. *Verh. Dtsch. Zool. Ges.* **66**:87–92.
24. KLEINOW, W., W. NEUPERT, and F. MILLER. 1974. Fine structure of mitochondrial ribosomes of locust flight muscle. *In* The Biogenesis of Mitochondria. A. M. Kroon and C. Saccone, editors. Academic Press Inc., New York and London. 337–346.

Downloaded from jcb.rupress.org on November 10, 2008